ARTICLE

Singlet Oxygen Phosphorescence Enhancement by Silver Islands Films[†]

Xavier Ragàs,[‡] Adaya Gallardo,[‡] Yongxia Zhang,[§] Walter Massad,[‡] Chris D. Geddes,[§] and Santi Nonell*,[‡]

[‡]Institut Químic de Sarrià, Universitat Ramon Llull, Via Augusta 390, 08017 Barcelona, Spain

[§]Institute of Fluorescence, Department of Chemistry & Biochemistry, University of Maryland Baltimore County, The Columbus Center, 701 East Pratt Street, Baltimore, Maryland 21202, United States

ABSTRACT: Optical detection of singlet oxygen, a reactive oxygen species that plays a crucial role in a variety of biomedical processes, is hampered by its extremely low emission probability. Using plasmonic effects induced in silver islands films coated with C_{60}, we have been able to enhance the near-IR phosphorescence of singlet oxygen by a factor of ca. 35. Both an enhanced production of singlet oxygen via plasmon-induced light absorption and the perturbation of its radiative rate constant are shown to account for this effect. The dependence of the enhancement factor on the properties of the silver island films and on the amount of C_{60} coated are discussed.
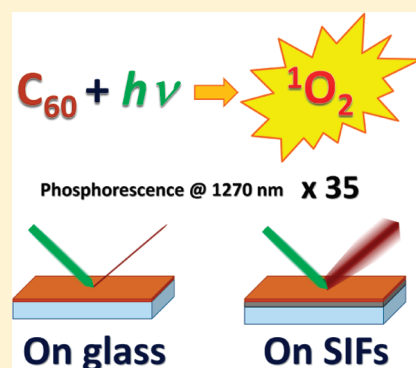
INTRODUCTION

Singlet molecular oxygen ($^1O_2$) is a reactive oxygen species (ROS) that participates in a variety of biological processes due to its ability to react with the molecules that make up many cellular components.[1] Detection of $^1O_2$ in biological environments with sufficient specificity, sensitivity, and temporal and spatial resolution remains a long sought-after goal, particularly in connection with the development of photodynamic therapy (PDT).[2,3] While it is relatively easy to detect $^1O_2$ indirectly through the use of spin traps,[4] chemical traps,[5] or fluorescent probes,[6−8] these are indirect detection techniques that make it very challenging to obtain mechanistic insight. A more direct approach is the monitoring of its phosphorescence at 1270 nm.[9] While this is regarded as the most direct and specific means of detecting $^1O_2$, it proves highly challenging due to an extremely low ($10^{-5}-10^{-7}$) emission quantum yield in biological media stemming from the overwhelming domination of nonradiative deactivation pathways.[10] Nonetheless, progress in the detection of $^1O_2$ phosphorescence in biological media is reported steadily, mainly as a result of technical developments in the photonics field.[2,3,9,11−13]

Over the past few years, it has been demonstrated that metallic surfaces, including colloids and islands, are able to induce significant changes on the emission properties of organic species.[14] Thus, processes such as metal-enhanced fluorescence (MEF)[15] and metal-enhanced phosphorescence (MEP)[16,17] have recently been described. Such effects can be explained by the interaction between excited luminophores and the surface plasmon electrons.[18]

It was just a matter of time that the $^1O_2$ community would turn its attention to the use of metallic surfaces to boost the phosphorescence of $^1O_2$. In fact, Toftegaard et al.[19] have recently

reported an enhancement of the radiative rate constant of $^1O_2$ by a factor of 3.5 by employing gold nanorods. It can be foreseen that improved nanomaterials will eventually be developed that will enhance further the radiative rate constant.

Radiative rate enhancement may not be the only, and perhaps not even the most important, effect of metal surfaces on singlet oxygen. Zhang et al. have recently demonstrated that silver island films (SIFs) enhance the production of singlet oxygen by a number of photosensitizers.[20] Interestingly, the extent of $^1O_2$ generation falls off exponentially with distance of the photosensitizer from the surface, suggesting that an enhanced excitation rate (enhanced absorbance cross-section) is the underlying mechanism for enhanced $^1O_2$ generation.[21]

In this paper we seek to gain a deeper insight into the photosensitizer-plasmon-oxygen photosystem by studying the effects of SIFs on the C_{60}-photosensitized $^1O_2$ phosphorescence at 1270 nm. C_{60} was chosen as photosensitizer since it produces $^1O_2$ with a quantum yield close to 1 in solution.[22]

EXPERIMENTAL SECTION

SIFs Preparation. SIFs with different sizes were prepared varying the deposition time and experimental conditions.[23,24] In a typical SIF preparation, a solution of silver nitrate (0.5 g in 60 mL of deionized water) was put in a clean 100-mL glass beaker. 200 μL of freshly prepared 5% (w/v) sodium hydroxide
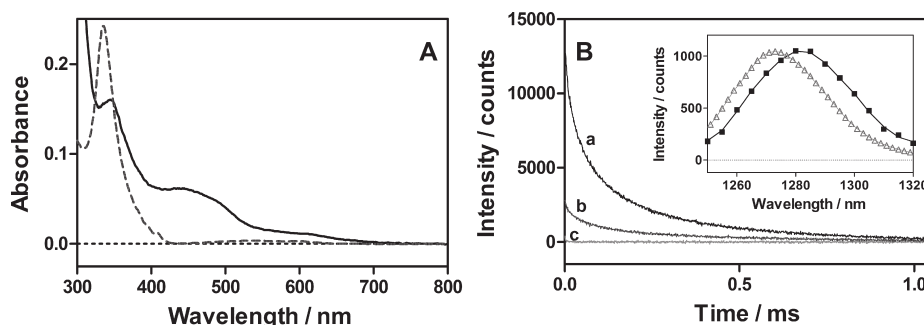
Figure 1. (A) Absorption spectrum of a C_{60} film on a glass slide (solid line) and C_{60} solution in toluene (dashed line). (B) Singlet oxygen phosphorescence at 1270 nm photosensitized by a C_{60} film coated on a glass slide upon irradiation at 532 nm. (a) Oxygen-saturated atmosphere. (b) Air-saturated atmosphere. (c) Argon-saturated atmosphere. Inset: Spectrum of the photoluminescence produced by a C_{60} film (squares) and by a C_{60} solution in toluene (triangles).

solution and 2 mL of ammonia were then added under continuous stirring at room temperature.

Subsequently, the solution was cooled to 5 °C by placing the beaker in an ice bath, followed by soaking Silane-prep glass slides (Fisher Scientific, Pittsburgh, PA) in the solution and adding a fresh solution of D-glucose (0.72 g in 15 mL of water). The mixture was then allowed to warm up to 30 °C. As the color of the mixture turned from yellowish green to yellowish brown, the slides were removed from the mixture, washed with water, and sonicated for 1 min at room temperature.

Scanning electron microscopy (SEM) micrographs were taken with a JEOL JSM 5310 microscope working at 20 kV.

C_{60} Film Formation. The C_{60} films were formed by spin coating C_{60} solutions (Sigma, St. Louis, MO, U.S.A.) at different concentrations (0.5, 1, 2, 3, 4, and 5 mg·mL^{-1}) in CS_2 (Sigma, St. Louis, MO, U.S.A.) by means of a KW-4A Spin Coater (SPI Supplies, West Chester, PA, U.S.A.) at 4000 rpm for 50 s.

Spectroscopic Measurements. Spectra were recorded on a Varian Cary 4E and Varian 6000i spectrophotometers. Three types of spectra were measured: (a) extinction spectra, defined as (eq 1)

$$E = 100 - CT \qquad (1)$$

where CT is the percentage of light transmitted along the beam direction in a conventional spectrophotometer; (b) reflectance spectra (R), obtained placing the sample after a 110 mm diameter integrating sphere, and (c) diffuse transmittance spectra (DT), obtained placing the sample before a 110 mm diameter integrating sphere. Absorption spectra (Abs) were then calculated by subtracting the reflectance (R) and diffuse transmittance (DT) spectra from 100% (eq 2):

$$Abs = 100 - DT - R \qquad (2)$$

Scattering spectra (S) were finally calculated by subtracting the extinction and absorption spectra (eq 3):

$$S = E - Abs \qquad (3)$$

Time-Resolved Singlet Oxygen Phosphorescence Measurements. Near-IR phosphorescence of $^1O_2$ was detected by means of a customized PicoQuant Fluotime 200 system described in detail elsewhere.[9] Briefly, a diode-pumped pulsed Nd:YAG laser (FTSS355-Q, Crystal Laser, Berlin, Germany) working at 10 kHz repetition rate at 532 nm (12 mW, 1.2 μJ per pulse)

Table 1. Luminescence Decay Kinetics Parameters at 1270 nm Produced by C_{60} Films Coated on SIFs Deposited for Increasing Amounts of Time and Exposed to Air upon Irradiation at 532 nm

preparation	atmosphere	$\tau_1/\mu s^a$	$\tau_2/\mu s^b$	$\tau_3/\mu s^c$
glass	air	534 ± 90	115 ± 8	10 ± 3
glass	O_2	420 ± 50	101 ± 5	23 ± 5
SIFs 1 min	air	445 ± 20	128 ± 4	22 ± 6
SIFs 2 min	air	442 ± 40	132 ± 9	31 ± 4
SIFs 4 min	air	500 ± 10	124 ± 10	24 ± 3
SIFs 6 min	air	613 ± 60	151 ± 33	34 ± 11
SIFs 8 min	air	641 ± 40	155 ± 27	40 ± 13

^{a} Relative amplitude 4.0 ± 1. ^{b} Relative amplitude 3.2 ± 1. ^{c} Relative amplitude 1.

was used for excitation. A 1064 nm rugate notch filter (Edmund Optics, U.K.) was placed at the exit port of the laser to remove any residual component of its fundamental emission in the near-IR region. The irradiated spot was 2×5 mm^2, as determined by a mask covering the samples. The luminescence exiting from the side of the sample was filtered by two long-pass filters of 355 and 532 nm (Edmund Optics, York, U.K.) and two narrow bandpass filters at 1270 nm (NB-1270-010, Spectrogon, Sweden; bk-1270-70-B, bk Interferenzoptik, Germany) to remove any scattered laser radiation. A near-IR sensitive photomultiplier tube assembly (H9170-45, Hamamatsu Photonics Hamamatsu City, Japan) was used as the detector at the exit port of the monochromator. Photon counting was achieved with a multichannel scaler (PicoQuant's Nanoharp 250). The time-resolved emission signals were analyzed using the PicoQuant FluoFit 4.0 data analysis software to extract the lifetime values.

The signals reported are the average of those obtained for four independent SIFs deposited for the same amount of time. Controls using either glass slides or SIFs without C_{60} (the PS) were carried out to confirm the lack of luminescence signal at 1270 nm due to $^1O_2$. Additionally, previously to the analysis, the same controls were subtracted from the signals produced by C_{60} films in order to remove any possible laser scattered light contribution to the signals.

■ RESULTS

C_{60} Films on Glass Slides. Figure 1A shows the absorption spectrum of the C_{60} film on glass and of C_{60} in toluene liquid
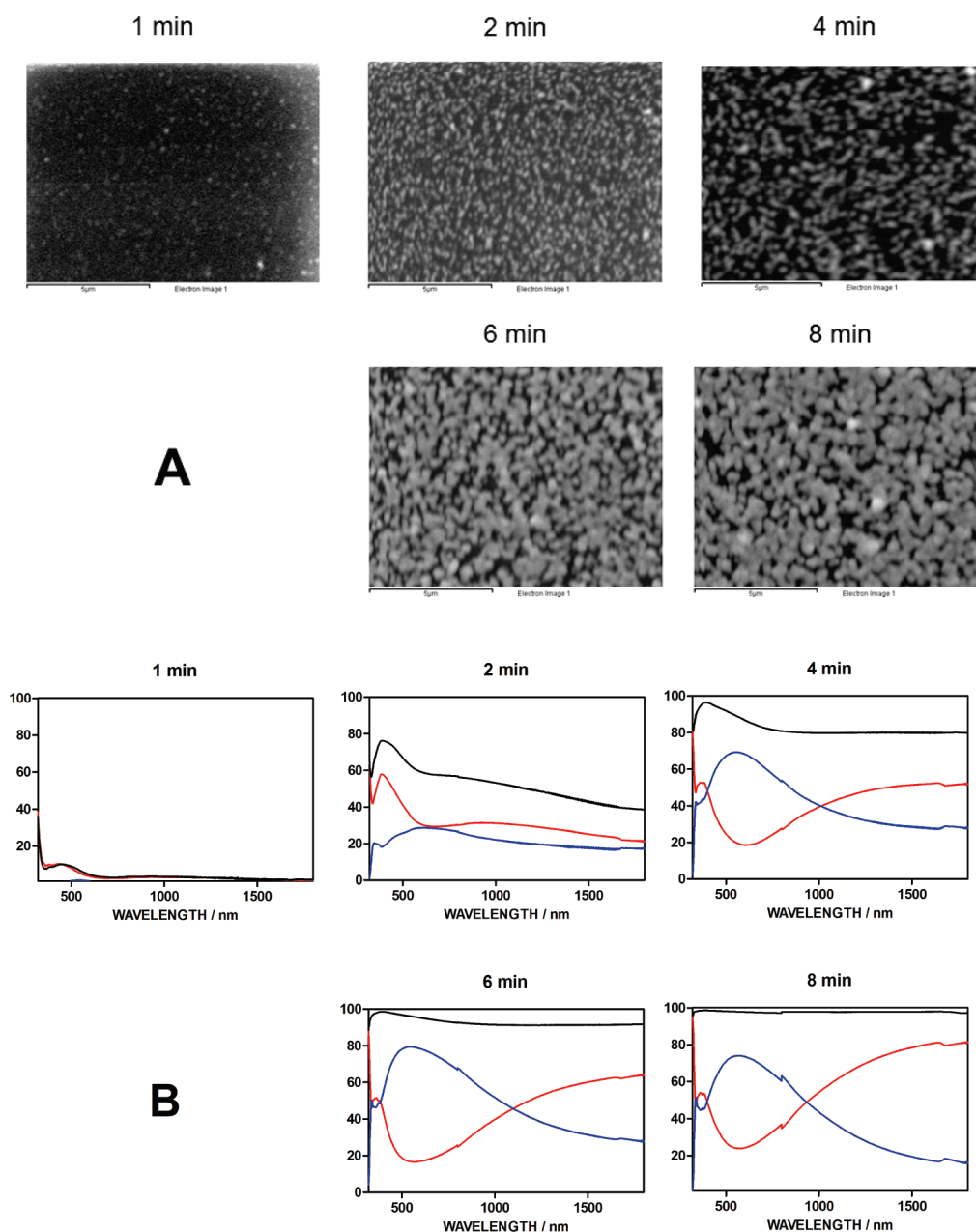
Figure 2. (A) SEM images of silver island films (SIFs) at 1, 2, 4, 6, and 8 min formation times. (B) Absorption (red), scattering (blue) and extinction (black) spectra of the SIFs.

solution. Clear differences are apparent, which resemble those described for $(C_{60})_n$ nanoclusters.[25] As shown in Figure 1B, the C_{60} film produced clear luminescence signals upon pulsed laser irradiation, which were unequivocally assigned to $^1O_2$ phosphorescence since they disappeared when either oxygen or C_{60} were excluded from the system. Interestingly, the maximum of the spectrum is red-shifted by ca. 10 nm relative to that observed in solution, indicating a highly polarizable microenvironment.[25] Also, the signal intensity increased proportionally to the partial pressure of oxygen in the gas phase, implying that a larger fraction of C_{60} triplets could be increasingly trapped by oxygen, and to the C_{60} concentration in solution, in agreement with the Beer—Lambert law for optically thin films. On the other hand, the phosphorescence decay deviated from the simple first-order kinetics typically observed in solution, requiring three exponential

terms to produce acceptable fits (Table 1). Taken together, all these observations are consistent with the formation of $(C_{60})_n$ nanoaggregates on the glass slide, probably similar to those observed in aqueous dispersions of C_{60}.[25]

C_{60} Films on SIFs. SIFs of different size and surface conditions were produced by growing the nanoparticles at different formation times.[24] Figure 2A shows the SEM images of the SIFs, that show that the size of the SIFs increase with the deposition time and that the distribution of the SIFs on the glass slide is rather homogeneous. Increasing the deposition time led to a blue shift in the absorption maxima with a concomitant increase in the absorption and scattering (Figure 2B). Similar observations have been reported by us recently, for SIFs of different size, silver-islands providing for a range of conditions for MEF.[23,24] In a recent paper, we have also reported both the wavelength
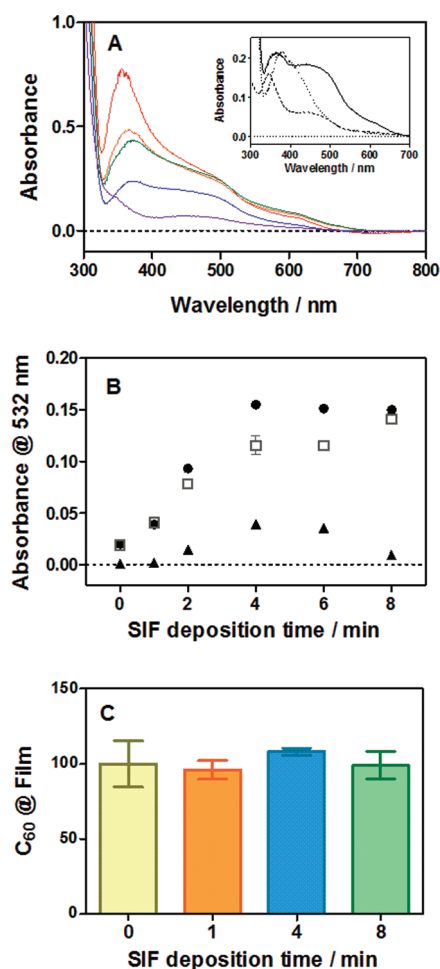
Figure 3. (A) Absorption spectra of SIFs spin-coated with C_{60} from a 3 mg·mL^{-1} solution. The spectra are not the simple sum of the individual SIF and C_{60} spectra. Inset: Absorption spectra of 2 min formation time SIFs spin-coated with C_{60} from a 3 mg·mL^{-1} solution (solid line), 2 min formation time SIFs alone (dotted line) and C_{60} film from a 3 mg·mL^{-1} solution (dashed line). (B) Absorbance at 532 nm produced by the SIFs-C_{60} system (circles), SIFs component (triangles), C_{60} component (squares). (C) Mean and SEM of the absorbance produced by the redisolution of the C_{60} films in toluene.

dependence of MEF as well as the effects of silver island size on enhanced fluorescence.[26] In these separate studies, larger silver islands are shown to enhance luminescence at longer wavelengths, which is deemed important for enhanced $^{1}O_{2}$ phosphorescence at 1270 nm as studied here. In the current study we have extended our observations to the near-infrared and found that scattering dominates in the visible region while absorption dominates in the near-infrared (Figure 2B).

When a C_{60} film was coated on the SIFs, the extinction spectrum of the resulting system showed all the features of the individual components. However the intensity of the C_{60} bands was enhanced in the green and red, but not in the blue, parts of the spectrum in a SIF deposition-time dependent manner (Figure 3A). Specifically, the absorbance of C_{60} at 532 nm, which one would expect to remain constant since the amount of C_{60} deposited was the same on all SIFs, increases linearly for short SIF deposition times and reaches a plateau for SIFs deposited for longest times (Figure 3B). Interestingly, no such enhancement is observed in the blue part of the spectrum. As shown in Figure 3C,

the amount of C_{60} coated is independent of the SIF deposition time, which confirms that the extinction enhancement is caused by the interaction between C_{60} and the SIFs. This is thought to be due to the change in refractive index above the SIFs by the C_{60} sample.

Enhancement of $^{1}O_{2}$ Phosphorescence by SIFs. As in the case of glass slides, C_{60} coated on the SIFs was also able to photosensitize $^{1}O_{2}$ upon irradiation at 532 nm (Figure 4A). The phosphorescence decay kinetics were very similar to those on glass slides, although a slight trend toward longer lifetimes can be observed upon increasing the SIF deposition time (Table 1). However, a major noticeable change is apparent, namely a large increase in the phosphorescence intensity (Figure 4A, inset), which is enhanced 18-fold on SIFs deposited for 2−4 min relative to the bare glass slides. SIFs deposited for shorter or longer times were less effective at enhancing the $^{1}O_{2}$ phosphorescence (Figure 4B). It is worth noting that the phosphorescence enhancement is, for several SIFs, larger than the absorbance enhancement observed at 532 nm. Moreover, both enhancements appear to be uncorrelated (Figure 4B). Interestingly no phosphorescence enhancement was observed when the films were irradiated at 355 nm.

$^{1}O_{2}$ Phosphorescence Stability and Reproducibility. The stability of the phosphorescence was measured as a function of the light dose received by the C_{60} films. To this end, the $^{1}O_{2}$ phosphorescence was collected over consecutive periods of 5 min each, always irradiating the same spot on the film. Figure 5A shows the evolution of the total $^{1}O_{2}$ luminescence after a series of irradiation cycles. While the signal remains stable for C_{60} films coated on bare glass slides, a substantial phosphorescence decrease is observed for the SIFs. However, when the irradiated C_{60} film was removed with organic solvents and new C_{60} was coated on the SIF, the original phosphorescence levels were recovered (Figure 5B).

Concentration Effects. In order to study the effects of the C_{60} concentration on the $^{1}O_{2}$ phosphorescence, SIFs were coated from solutions of C_{60} concentration ranging from 0.5 to 5 mg mL^{-1}. As observed from the $^{1}O_{2}$ phosphorescence traces in the inset of Figure 6A, the decay kinetics were not affected by the amount of C_{60} deposited. However, the intensity of the signal increased, as in the case of glass slides, although clear differences are apparent (Figure 6B). At low C_{60} concentrations, the slope of the total luminescence-vs-concentration plot is larger than that observed for glass slides, while equal slopes are observed at the highest concentrations. These data reveal a clear concentration effect on the phosphorescence enhancement. As depicted in Figure 6C, SIFs deposited for 2 min show a 32-fold phosphorescence enhancement factor for C_{60} concentrations up to 1 mg mL^{-1} and a clear downward trend at higher concentrations.

■ DISCUSSION

The application of plasmon-coupling effects to boost the phosphorescence of $^{1}O_{2}$ is of potential interest from a fundamental point of view and also for the monitoring of this reactive oxygen species in biological media. Our studies clearly demonstrate that SIFs can be successfully applied to this end, with observed $^{1}O_{2}$ phosphorescence enhancement factors up to 35 fold, 1 order of magnitude larger than the 3.5 factor reported so far for gold nanorods.[19] Potential causes for such a $^{1}O_{2}$ phosphorescence enhancement are either a higher production of $^{1}O_{2}$ or a higher probability for $^{1}O_{2}$ radiative decay, or both.
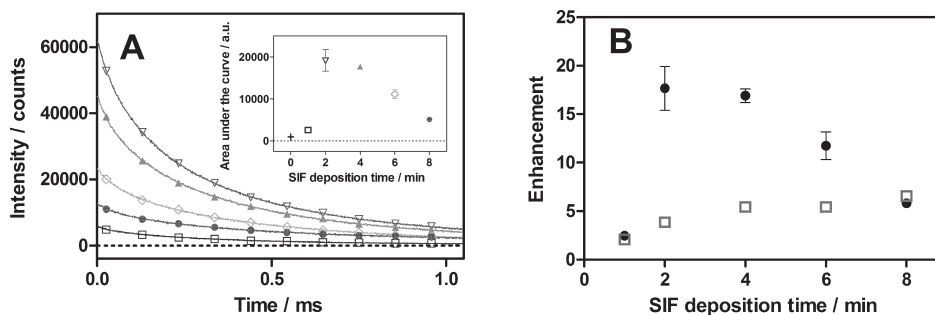
Figure 4. Effect of the silver island size on the singlet oxygen luminescence. (A) Singlet oxygen kinetics as a function of the silver island formation time: 1 (squares), 2 (inversed triangles), 4 (triangles), 6 (diamonds), and 8 min (circles). The concentration of C_{60} was 3 mg mL^{-1} and the excitation wavelength was 532 nm. Inset: Area under the singlet oxygen luminescence curves produced by C_{60} films coating SIFs and a C_{60} film (cross). (B) Enhancement of the singlet oxygen luminescence signal (circles) and the absorption factor at 532 nm (squares) observed with SIFs at different formation times with a 3 mg mL^{-1} concentration of C_{60}.
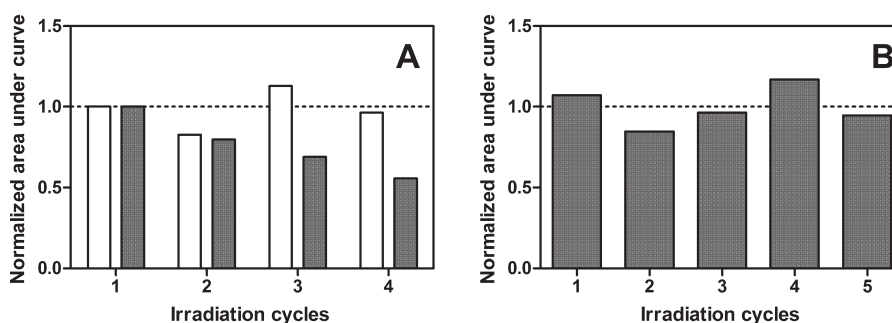
Figure 5. Stability and reproducibility of the singlet oxygen luminescence produced by C_{60}-coated SIFs from a 3 mg mL^{-1} C_{60} solution and 2 min deposition time upon irradiation at 532 nm. (A) Normalized area under the decay curve vs. number of irradiation cycles (5 min each) for C_{60} films coated on glass slides (white) or silver islands (black). (B) Same as in panel A but with a C_{60} film freshly coated after each cycle.

As to the first possibility, it must be born in mind that production of $^1O_2$ is based on the photosensitization process, i.e., absorption of light energy renders C_{60} in its singlet electronically excited state ($^1C_{60}{}^*$), from which it undergoes intersystem crossing to the longer-lived triplet state ($^3C_{60}{}^*$). Production of $^1O_2$ then occurs by energy transfer from $^3C_{60}{}^*$ to nearby oxygen molecules in a diffusion-controlled process (Scheme 1). In air-saturated solutions, both the formation of $^3C_{60}{}^*$ and energy transfer to oxygen occur with ca. 100% efficiency, resulting in a quantum yield of $^1O_2$ production (Φ_Δ) close to 1.[22]

It is thus apparent that an enhanced production of singlet oxygen will occur if light absorption by C_{60}, or $^1C_{60}{}^* \rightarrow {}^3C_{60}{}^*$ intersystem crossing, or energy transfer to oxygen are enhanced by the SIFs.

Our results clearly show that an enhanced plasmon-induced absorption of light is indeed taking place at 532 nm but not at 355 nm (Figure 2, panels B and C), in agreement with earlier reports.[26] However, the trends in absorption and $^1O_2$ phosphorescence enhancement are uncorrelated (Figure 4B), therefore additional contributions must be considered. As to the C_{60} photophysics, the triplet quantum yield is already 1 in solution and the results by Byrne et al. indicate that the C_{60} molecule is minimally perturbed in the solid state.[28] This allows us to reasonably assume that the triplet quantum yield is also close to 1 in the films, ruling out an enhanced $^1C_{60}{}^* \rightarrow {}^3C_{60}{}^*$ intersystem crossing.

The possibility that the SIFs enhance the transfer of energy from $^3C_{60}{}^*$ to oxygen must be examined. The observation that

the $^1O_2$ phosphorescence intensity increases ca. 5-fold when both the glass and the SIFs samples are exposed to pure oxygen relative to air, indicates an inefficient trapping of $^3C_{60}{}^*$ by oxygen in all cases. This effect, observed previously for $(C_{60})_n$ nano-aggregates,[25] indicates a low permeability of oxygen into the C_{60} film. It is unlikely that this is changed by the nature of the underlying substrate, be it bare glass or the SIFs. The reproducibility of the conditions used for spin-coating, demonstrated by the fact that all films contained the same amount of C_{60} (Figure 3C) allow us to assume that the mobility of oxygen in the films, and therefore the fraction of C_{60} triplets trapped by oxygen, will be comparable in all preparations, thus ruling out any substantial enhancement of the energy-transfer process by the SIFs.

In the light of the preceding discussion, the results in Figure 4B lead us to conclude that an enhanced production of $^1O_2$, as a result of a higher plasmon-induced light absorption, is the main underlying cause for $^1O_2$ phosphorescence enhancement for both the smallest and largest SIFs tested in this work. However a comparison between the phosphorescence and light-absorption enhancements (Figure 4B) also indicates that the $^1O_2$ radiative decay rate constant is enhanced as well by the SIFs. Consistent with this, we find that the SIFs show substantial absorption and scattering components at 1280 nm (Figure 2B)

The C_{60} concentration effects shown in Figure 6 provide additional evidence for the conclusions above. The current understanding of plasmonic coupling and enhancing effects predict that such effects are extended only through a few nanometers
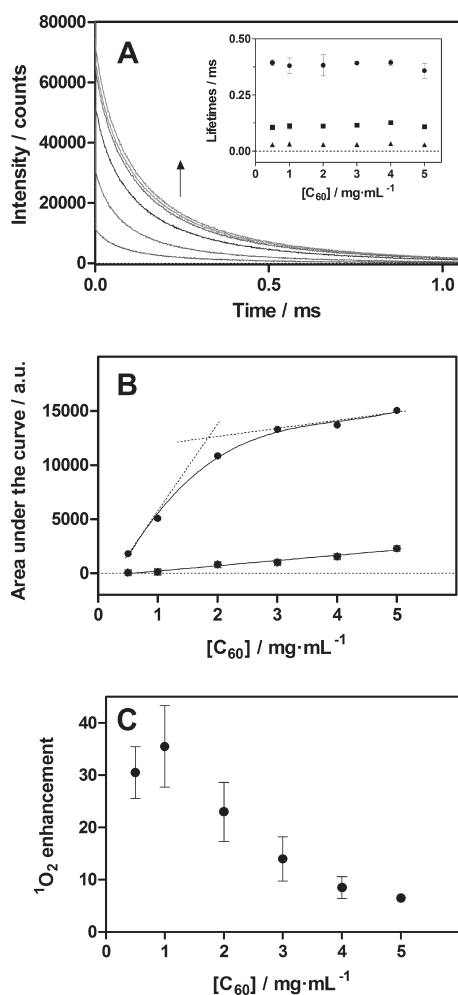
Figure 6. Effect of the concentration of C_{60} (0.5, 1, 2, 3, 4, and 5 $mg \cdot mL^{-1}$) on the 1270-nm singlet oxygen phosphorescence from silver islands films upon irradiation at 532 nm. (A) Singlet oxygen kinetics on a 2 min silver island film at increasing concentrations of C_{60}. Inset: Lifetimes of the three components observed for the singlet oxygen luminescence signals. (B) Area under the singlet oxygen luminescence curves for C_{60} films on SIFs (circles) and on glass slides (squares). (C) Enhancement of the singlet oxygen luminescence signal observed with increasing concentrations of C_{60}.

Scheme 1

$$C_{60} + h\nu \rightarrow {}^1C_{60}{}^* \rightarrow {}^3C_{60}{}^*$$
$${}^3C_{60}{}^* + O_2 \rightarrow C_{60} + {}^1O_2$$
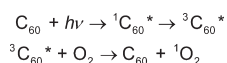
from the nanoparticles.[20] Consistent with this, a roughly constant (32 ± 5)-fold $^1O_2$ phosphorescence enhancement factor is observed at low C_{60} loadings. However as additional C_{60} layers are deposited the enhancement levels off, reflecting that the newly deposited molecules are too far away from the SIFs to sense their plasmonic effects.

Finally, it is interesting to comment on the observation that the phosphorescence of $^1O_2$ decreases when the number of irradiation cycles is increased. At first one may consider the oxidation of the SIFs and the concomitant loss of plasmon resonance to be the explanation. However, as shown in Figure 5B, fresh coatings of C_{60} films provide for very similar phosphorescence signals.

This suggests that the surface remains unperturbed and that the amount of $^1O_2$ molecules decreases as the number of cycles is increased, due to C_{60} film transformation, e.g., by self-photooxidation. Given the enhanced absorption cross sections, coupled with the significant generation of $^1O_2$, then this result is not surprising.

CONCLUSIONS

In this paper we have shown that silver-surface plasmons are efficient enhancers of $^1O_2$ phosphorescence as monitored directly at 1270 nm. Interestingly, our approach offers for up to a 35—fold increase in $^1O_2$ generation as compared to control samples which do not contain plasmon supporting materials, which is of significance for both the study and utility of $^1O_2$ in the biosciences. Thus, on one hand, this enhancement would allow the measurement of $^1O_2$ kinetics in biological systems using shorter periods of time, or even open the possibility to boost the detection of this reactive oxygen species in vivo. On the other hand, it would allow a reduction of the light-dose or the drug-dose in PDT treatments, or would increase the effectiveness of commonly used PSs by conjugation of nanoparticles with ability to produce such plasmonic effect with commonly used photosensitizers.

AUTHOR INFORMATION

Corresponding Author
*Telephone: +34 932672000. Fax: +34 932056266. E-mail: santi.nonell@iqs.url.edu.

ACKNOWLEDGMENT

DEDICATION

[†]Dedicated to the memory of Prof. Roberto Sastre.

REFERENCES

(1) Wilkinson, F.; Helman, W. P.; Ross, A. B. *J. Phys. Chem. Ref. Data* **1995**, *24*, 663.
(2) Jimenez-Banzo, A.; Sagrista, M. L.; Mora, M.; Nonell, S. *Free Radical Biol. Med.* **2008**, *44*, 1926.
(3) Ragas, X.; Agut, M.; Nonell, S. *Free Radical Biol. Med.* **2010**, *49*, 770.
(4) Hideg, E.; Spetea, C.; Vass, I. *Photosynth. Res.* **1994**, *39*, 191.
(5) Telfer, A.; Bishop, S. M.; Phillips, D.; Barber, J. *J. Biol. Chem.* **1994**, *269*, 13244.
(6) Ragas, X.; Jimenez-Banzo, A.; Sanchez-Garcia, D.; Batllori, X.; Nonell, S. *Chem. Commun.* **2009**, *20*, 2920.
(7) Flors, C.; Fryer, M. J.; Waring, J.; Reeder, B.; Bechtold, U.; Mullineaux, P. M.; Nonell, S.; Wilson, M. T.; Baker, N. R. *J. Exp. Bot.* **2006**, *57*, 1725.
(8) Tanaka, K.; Miura, T.; Umezawa, N.; Urano, Y.; Kikuchi, K.; Higuchi, T.; Nagano, T. *J. Am. Chem. Soc.* **2001**, *123*, 2530.
(9) Jimenez-Banzo, A.; Ragas, X.; Kapusta, P.; Nonell, S. *Photochem. Photobiol. Sci.* **2008**, *7*, 1003.
(10) Schweitzer, C.; Schmidt, R. *Chem. Rev.* **2003**, *103*, 1685.

(11) Maisch, T.; Baier, J.; Franz, B.; Maier, M.; Landthaler, M.; Szeimies, R. M.; Baumler, W. *Proc. Natl. Acad. Sci. U.S.A.* **2007**, *104*, 7223.

(12) Breitenbach, T.; Kuimova, M. K.; Gbur, P.; Hatz, S.; Schack, N. B.; Pedersen, B. W.; Lambert, J. D. C.; Poulsen, L.; Ogilby, P. R. *Photochem. Photobiol. Sci.* **2009**, *8*, 442.

(13) Codling, C. E.; Maillard, J. Y.; Russell, A. D. *J. Antimicrob. Chemother.* **2003**, *51*, 1153.

(14) Lakowicz, J. R. *Anal. Biochem.* **2001**, *298*, 1.

(15) Geddes, C. D.; Lakowicz, J. R. *J. Fluoresc.* **2002**, *12*, 121.

(16) Zhang, Y. X.; Aslan, K.; Malyn, S. N.; Geddes, C. D. *Chem. Phys. Lett.* **2006**, *427*, 432.

(17) Zhang, Y. X.; Aslan, K.; Previte, M. J. R.; Malyn, S. N.; Geddes, C. D. *J. Phys. Chem. B* **2006**, *110*, 25108.

(18) Lakowicz, J. R. *Anal. Biochem.* **2005**, *337*, 171.

(19) Toftegaard, R.; Arnbjerg, J.; Daasbjerg, K.; Ogilby, P. R.; Dmitriev, A.; Sutherland, D. S.; Poulsen, L. *Angew. Chem., Int. Ed.* **2008**, *47*, 6025.

(20) Zhang, Y.; Aslan, K.; Previte, M. J. R.; Geddes, C. D. *Proc. Natl. Acad. Sci. U.S.A.* **2008**, *105*, 1798.

(21) Geddes, C. D. Metal-Enhanced Fluorescence: Progress Towards a Unified Plasmon Fluorophore Description. In *Metal-Enhanced Fluorescence*; John Wiley and Sons: New York, 2010; pp 1—24.

(22) Arbogast, J. W.; Darmanyan, A. P.; Foote, C. S.; Rubin, Y.; Diederich, F. N.; Alvarez, M. M.; Anz, S. J.; Whetten, R. L. *J. Phys. Chem.* **1991**, *95*, 11.

(23) Aslan, K.; Leonenko, Z.; Lakowicz, J. R.; Geddes, C. D. *J. Fluoresc.* **2005**, *15*, 643.

(24) Pribik, R.; Dragan, A. I.; Zhang, Y.; Gaydos, C.; Geddes, C. D. *Chem. Phys. Lett.* **2009**, *478*, 70.

(25) Bilski, P.; Zhao, B. Z.; Chignell, C. F. *Chem. Phys. Lett.* **2008**, *458*, 157.

(26) Zhang, Y.; Dragan, A.; Geddes, C. D. *J. Phys. Chem. C* **2009**, *113*, 12095.

(27) Ma, B.; Sun, Y.-P. *J. Chem. Soc. Perkin Trans. 2* **1996**, *10*, 2157.

(28) Byrne, H. J.; Maser, W. K.; Kaiser, M.; Akselrod, L.; Anders, J.; Ruhle, W. W.; Zhou, X. Q.; Thomsen, C.; Werner, A. T.; Mittelbach, A.; Roth, S. *J. Mat. Process. Technol.* **1995**, *54*, 149.

16281

dx.doi.org/10.1021/jp202095a |*J. Phys. Chem. C* 2011, 115, 16275—16281